SCIENTIFIC REPORTS

SUBJECT AREAS:
STRESS SIGNALLING
BIOCHEMICAL NETWORKS
MICROARRAYS
CELLULAR SIGNALLING NETWORKS

Received
14 December 2012

Accepted
2 May 2013

Published
23 May 2013

Correspondence and requests for materials should be addressed to M.A.C. (macarlso@unmc.edu)

Attachment-regulated signaling networks in the fibroblast-populated 3D collagen matrix

Mark A. Carlson[1,4], Lynette M. Smith[2], Crystal M. Cordes[3], Jie Chao[1] & James D. Eudy[4]

[1]Departments of Surgery, VA Nebraska–Western Iowa Health Care System and the University of Nebraska Medical Center, Omaha, NE 68105, USA, [2]Biostatistics Department, University of Nebraska Medical Center, Omaha, NE 68198-4375 USA, [3]Department of Obstetrics and Gynecology, University of Nebraska Medical Center, Omaha, NE 68198-3255 USA, [4]Department of Genetics, Cell Biology and Anatomy, University of Nebraska Medical Center, Omaha, NE 68198-5915 USA.

Fibroblasts in the attached collagen matrix are in a pro-survival, pro-proliferative state relative to fibroblasts in the released collagen matrix, such that matrix cell number increases in the former over time. Gene array data from attached *vs.* released matrices were analyzed for putative networks that regulated matrix cell number. Select networks then underwent augmentation and/or inhibition in order to determine their biologic relevance. Matrix stress-release was associated with modulation of signaling networks that involved IL6, IL8, NF-κB, TGF-β1, p53, interferon-γ, and other entities as central participants. Perturbation of select networks in multiple fibroblast strains suggested that IL6 and IL8 secretion may have been involved in preservation of matrix cell population in the released matrix, though there was variability in testing results among the strains. NF-κB activation may have contributed to the induction of population regression after matrix release.

The three-dimensional fibroblast-populated collagen matrix (FPCM) model was developed in the late 1970's as a skin equivalent for dermal replacement therapy[1–3]. A derivative of this model has been used successfully to treat patients with massive (>60% total body surface area) full-thickness burn injury[4]. Currently, the FPCM is used to study a wide range of cell types in a three-dimensional environment; when populated with primary dermal fibroblasts, the collagen matrix has been used as a model of dermal healing and wound contraction[5,6]. Overall, 3D collagen matrix systems have had an increasing role in the field of tissue engineering[7–10].

One application of the FPCM is to study the effects of matrix anchorage on the fate of cells within the matrix[3]. Fibroblasts in a collagen matrix that is attached to the culture surface are in a pro-survival, pro-proliferative state relative to fibroblasts in a matrix that has been detached (stress-released) from the culture surface and is floating freely in the medium[5,11–13]. The net result of this situation is that matrix cell number increases in the attached matrix over time. Work by others has implicated a role in perturbation of the RAS-RAF-MEK-MAPK axis[14–16] and the β1-integrin-FAK-PI-3-kinase-Akt axis[17,18] in the modulation of cell fate in relaxed matrices; PTEN[19] and ILK (integrin-linked kinase)[20] also may be involved. It was our intent in this study to compare gene expression in attached *vs.* stress-released matrices in order to uncover new/additional signaling networks that regulate matrix cell number, and then to perform preliminary relevance testing on some of these networks.

Results

DNA microarrays of attached *vs.* released matrices. The FPCM model[5,6,21,22] and its morphologic parallels with an animal wound model[23–25] are reviewed in Supplementary Figures S1–S4. An index DNA array experiment (see Supplementary Figure S5 for summary flow diagram) was defined as the comparison of gene expression in attached *vs.* stress-released collagen matrices (Supplementary Figure S1) in a single strain of human foreskin fibroblasts at 6 and 24 h after matrix release. The selection of the 6 and 24 h time points was based on published data[5]. Each comparison was done using a 10 K spotted gene chip (GSE39475[26]). Index experiments were performed on three fibroblast strains, meaning that expressional data were derived from three foreskin donors (nonpooled samples). Unless otherwise specified, "released" in this manuscript refers to "stress-released"[3], i.e., detachment of an attached matrix which has had sufficient time (>24 h) to generate pre-stress.

After screening the microarrays for problematic spots (e.g., bad morphology or aberrant hybridization), data was available for 8,693 genes. All genes that were differentially expressed (defined as "DE genes"; see Materials

and Methods) in the 6 and 24 h analyses are given in Supplementary Tables S1 and S2, respectively. There were 187 and 423 DE genes at the 6 and 24 h time points, respectively; 99% of these genes met the distributional assumptions of the Kolmogorov Goodness-of-Fit test. A selection of these DE genes is shown in Tables 1 and 2 (from the 6 and 24 h time points, respectively). The genes which had a significant change in relative expression (released/attached) over time, i.e., between the 6 and 24 h time points, are shown in Supplementary Table S3. It should be noted, however, that the gene chip experiment was not designed to detect expression differences between the 6 and 24 h time points (see discussion accompanying Supplementary Table S3).

Corroboration of select DE genes with qPCR, ELISA, and immunoblotting. DE genes identified at the 24 h time point included cyclin B2, GADD45α, GAPDH, IL-6, IL-8, and PCNA (Table 2). The results of quantitative PCR (qPCR) of the transcripts for these genes are shown in Table 3. With the exception of GADD45α, the change in gene expression for this subset of genes in attached *vs.* released matrices was consistent with the microarray results. The qPCR data revealed a trend of GADD45α upregulation in the released matrices (directional change consistent with the array data), but this was not statistically significant. So for this small selection of DE genes, qPCR confirmed the microarray results.

ELISA for IL-6 or IL-8 in the medium of attached *vs.* released matrices indicated that both of these cytokines were induced after matrix release (Figure 1), which was consistent with the array data (Tables 1 and 2). The level of both IL-6 and IL-8 in growth medium not exposed to cells was < 150 pg/mL (data not shown). ELISAs performed on media harvested 6 h after release did not consistently demonstrate a change in IL-6 or IL-8 concentration after matrix release (data not shown). ELISAs performed at 24 and 48 h after release, however, revealed that both IL-6 and IL-8 increased in the medium of the released matrix with respect to the attached matrix (Figure 1), which was consistent with the microarray results. Immunoblotting for the intracellular proteins of select DE genes is shown in Supplementary Figure S6; these data mostly confirmed the array data. In addition, a comparison of the array data obtained from the present report with a historical dataset is given in Supplementary Figure S7.

Construction of putative networks from the DE gene list. The set of DE genes in Supplementary Tables S1 and S2 were analyzed with proprietary software (Ingenuity® Pathways Analysis version 6, IPA® 6; www.ingenuity.com), and putative networks of gene products likely modulated between the attached *vs.* released states of the FPCM were constructed. This software inspects expressional data for relationships among DE genes, drawing from a proprietary database that contains millions of annotated relationships between proteins, genes, complexes, and other entities[27,28]. Essentially, the program extracts higher-order relationships from a ranked list of expressional data (e.g., the DE genes listed in Supplementary Tables S1 and S2).

The IPA® software analysis identified 8 and 18 putative networks (Supplementary Figure S8) at the 6 and 24 h time points, respectively, that may have been modulated between the attached vs. released states of the FPCM. A partial list of these networks along with presumed functions (also generated by the software) is given in Table 4. Common functions of the networks identified in this analysis included cell death and the cell cycle, which was consistent with

Table 1 | Select genes differentially expressed in the released with respect to the attached FPCM at 6 h

Selected genes OVERexpressed in released with respect to attached matrices (6 h)		
ID	Description	Mean fold change (rel/att)
NM_000600_1	interleukin 6 (interferon, beta 2); IL-6	4.428
NM_001200_1	bone morphogenetic protein 2 precursor; BMP2	3.158
NM_004052_1	Bcl-2/adenovirus E1B 19 kDa-interacting protein 3; BNIP3	3.207
NM_002923_1	regulator of G-protein signaling 2, 24 kDa; RGS2	2.297
NM_000432_1	myosin light chain 2; MLC-2	2.253
NM_003028_1	Shb adaptor protein (a Src homology 2 protein); Shb	2.111
NM_004292_1	Ras inhibitor; RIN1	2.305
NM_003275_1	tropomodulin	2.378
NM_002425_1	matrix metalloproteinase 10; MMP-10	2.297
NM_002178_1	insulin-like growth factor binding protein 6; IGFBP-6	2.366
NM_005384_1	nuclear factor, interleukin-3 regulated; NFIL3	2.180
NM_004794_1	Rab33A, member Ras oncogene family	2.190
NM_012094_1	peroxiredoxin 5; PRDX5	2.036
NM_000577_1	interleukin 1 receptor antagonist; IL-1Ra	2.343
Selected genes UNDERexpressed in released with respect to attached matrices (6 h)		
ID	Description	Mean fold change (rel/att)
NM_012242_1	DKK1	0.209
NM_001901_1	connective tissue growth factor; CTGF	0.330
NM_001709_1	brain-derived neurotrophic factor; BDNF	0.422
NM_025239_1	programmed death ligand 2; PDL2	0.450
NM_004161_1	Rab1, member Ras oncogene family; Rab1	0.494
NM_000615_1	neural cell adhesion molecule 1; NCAM1	0.353
NM_006449_1	Cdc42 effector protein 3; CEP3	0.424
NM_006911_1	relaxin 1	0.478
NM_005610_1	retinoblastoma-binding protein 4; RBP4	0.494
NM_004330_1	Bcl-2/adenovirus E1B 19 kDa-interacting protein 2; BNIP2	0.453
NM_002592_1	proliferating cell nuclear antigen; PCNA	0.491
NM_002890_1	Ras p21 protein activator 1, isoform 1; RASA1	0.490

rel/att = released/attached. All genes listed have a significance of $p < 0.001$. Genes were selected from the 6 h DE gene list (N = 185; see Supplementary Table S1), in which mean fold change was >2 or <0.5.

Table 2 | Select genes differentially expressed in the released with respect to the attached FPCM at 24 h

Selected genes OVERexpressed in released with respect to attached matrices (24 hr)		
ID	Description	Mean fold change (rel/att)
NM_000600_1	interleukin 6 (interferon, beta 2); IL-6	11.20
NM_002425_1	matrix metalloproteinase 10 preproprotein; MMP-10	17.95
NM_000584_1	interleukin 8; IL-8	10.17
NM_000576_1	interleukin 1, beta; IL-1β	5.44
NM_001924_1	growth arrest and dna-damage-inducible, alpha; GADD45α	3.71
NM_000577_1	interleukin 1 receptor antagonist; IL-1Ra	3.61
NM_004052_1	Bcl-2/adenovirus E1B 19 kDa-interacting protein 3; BNIP3	4.13
NM_002923_1	regulator of G-protein signaling 2, 24 kDa; RGS2	2.54
NM_006835_1	cyclin I; CCNI	2.39
NM_004049_1	Bcl2-related protein a1; BCL2A1	2.91
NM_001256799_1	glyceraldehyde-3-phosphate dehydrogenase (GAPDH)	3.02
NM_001401_1	lysophosphatidic acid receptor EDG2	2.15
NM_000432_1	myosin light chain 2; MLC-2	2.63
NM_003789_1	TNFRSF1A-associated via death domain; TRADD	2.19
NM_000636_1	superoxide dismutase 2, mitochondrial; SOD2	2.43
NM_002178_1	insulin-like growth factor binding protein 6; IGFBP-6	2.37
NM_002659_1	plasminogen activator, urokinase receptor; PLAUR	2.04
NM_004050_1	Bcl2-like 2 protein; BCL2L2	2.44
Selected genes UNDERexpressed in released with respect to attached matrices (24 hr)		
ID	Description	Mean fold change (rel/att)
NM_002416_1	monokine induced by gamma interferon; MIG	0.262
NM_002692_1	polymerase (DNA directed), epsilon 2; POLE2	0.288
NM_002592_1	proliferating cell nuclear antigen; PCNA	0.292
NM_004701_1	cyclin B2; CCNB2	0.315
NM_005192_1	cyclin-dependent kinase inhibitor 3; CDKN3	0.324
NM_001786_1	cell division cycle 2 protein, isoform 1; CDC2	0.341
NM_004208_1	programmed cell death 8 (apoptosis-inducing factor); PDCD8	0.356
NM_033293_1	caspase 1, isoform gamma precursor; CASP1	0.363
NM_006644_1	heat shock 105 kDa; HSP105B	0.404
NM_012333_1	c-Myc binding protein; MYCBP	0.417
Y10658_1	nuclear DNA helicase II	0.428
NM_000366_1	tropomyosin 1 (alpha)	0.441
NM_000800_1	fibroblast growth factor 1 (acidic), isoform 1 precursor; FGF-1	0.449
NM_001709_1	brain-derived neurotrophic factor; BDNF	0.459
NM_001165_1	baculoviral IAP repeat-containing protein 3; BIRC3	0.504
NM_025239_1	programmed death ligand 2; PDL2	0.443
NM_004282_1	Bcl2-associated athanogene 2; BAG2	0.388

rel/att = released/attached. All genes listed have a significance of $p < 0.001$. Genes were selected from the 24 h DE gene list (N = 425; see Supplementary Table S2), in which mean fold change was >2 or <0.5.

the known biology of the collagen matrix model[5] (Supplementary Figures S1 and S9). Canonical biofunctions and signaling pathways that were identified by the software analysis as having been modulated are described in Supplementary Figure S10 and Supplementary Tables S6–S9.

Two networks from Supplementary Figure S8 are reproduced for further comment in Figure 2. The central participants in network 6–2 (Figure 2a) were IL6, PCNA, Histone H3, cyclins, and MEK 1/2. A putative function associated with this network was cell cycle regulation (Table 4). The post-release modulation of IL6 and PCNA (Figure 1 and Supplementary Figure S6) was consistent with the putative network shown in Figure 2a. The central participants in network 24–15 (Figure 2b) included p53 and NOS3; the putative functions of this network were regulation of the cell cycle, DNA replication/recombination/repair, and cell death. Of note, p53 itself was not a DE gene (Supplementary Tables S1 and S2). Previous descriptions of p53 regulation have focused post-translational modifications that can enhance and/or reduce p53 activity and promote

Table 3 | Relative expression of select DE genes by qPCR in the attached *vs.* released FPCM

Gene	6 h Att	6 h Rel	24 h Att	24 h Rel
cyclin B2	1.02 ± 0.04	0.93 ± 0.09	0.83 ± 0.11	0.35 ± 0.04*
GADD45α	1.12 ± 0.11	1.55 ± 0.15	1.13 ± 0.12	1.36 ± 0.24
GAPDH	1.03 ± 0.05	1.14 ± 0.08	1.24 ± 0.07	1.74 ± 0.16*
IL6	4.17 ± 1.35	19.31 ± 4.39	17.55 ± 6.19	80.05 ± 22.18*
IL8	1.26 ± 0.19	2.30 ± 0.63	3.48 ± 0.85	39.51 ± 9.56*
PCNA	1.03 ± 0.06	0.73 ± 0.06*	0.87 ±0.04	0.70 ± 0.04*

Att = attached; Rel = released. Values are relative gene expression (mean ± SD) with respect to the standard (TATA box binding protein); *$p < 0.05$ compared to the 6 h attached value (ANOVA and the unpaired t-test).

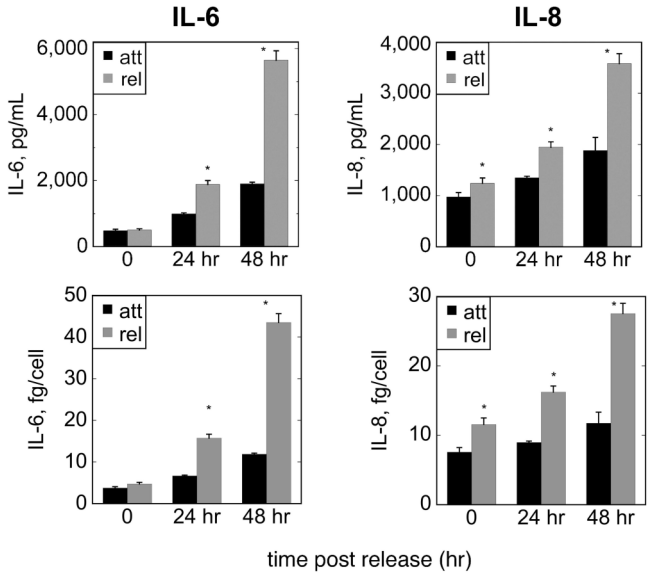

Figure 1 | ELISA corroboration of microarray data. ELISA of IL6 and IL8 in the culture media of attached (att) *vs.* released (rel) collagen matrices at 0–48 hr post release. Each data bar represents the mean of quadruplicate tubes; error bars represent standard deviations. This particular experiment was performed in four different cells strains with similar results. Upper panels represent raw data (cytokine concentration in the medium); lower panels represent cytokine release normalized to cell number. *$p < 0.05$ compared to attached at same time point, unpaired t-test.

and/or inhibit p53 turnover[29–32]. So the fact that a p53-centric network was implicated by our microarray data in the absence of differential p53 expression should not be surprising. Immunoblotting for products of other non-DE genes which were central participants in various networks of Supplementary Figure S8 is shown in Supplementary Figure S11.

In order to determine whether the level of the p53 protein actually was modulated in our system, p53 immunoblotting was performed in lysates of attached *vs.* released matrices (Figure 2c–d). The p53 level appeared to be increased in the attached matrix at 6 h, but then is increased in the released matrix at 24 h. Since previous work suggested that the p53 response in this system is subject to biologic (strain-to-strain) variability[33], the immunoblot shown in Figure 2c was repeated in 11 different fibroblast strains; the result at 6 h was variable, but p53 upregulation in the released matrix at 24 h was present in 8 out of 11 strains. This result suggested that p53 generally is induced after matrix release, particularly at the 24 h time point. The modulation of the p53 protein after matrix release was consistent with the putative p53-centric network shown in Figure 2b.

Effect of modulation of putative networks. The IPA® 6 analysis predicted that networks with IL-6, IL-8, p53, TGF-β1, NF-κB, or interferon-gamma (IFN-γ) as central participants would regulate cell survival and/or the cell cycle after stress-release of the FPCM (see Table 4 and Supplementary Figure S8). In order to test these predictions, the effects of relevant soluble inhibitors/activators on matrix cell number were assayed. The basic design of the inhibitor/activator experiments was pretreatment of the attached matrix with a range of doses of a given reagent, followed by matrix release in half of the wells, and then measurement of cells per matrix 48 and 72 h later.

The effects of 14 reagents/reagent combinations were tested on 3 to 16 fibroblast strains per reagent, resulting in over 200 individual experiments on the FPCM. Two typical experiments from this series, showing the effect of fetal bovine serum or pifithrin-μ (a small molecule inhibitor of p53[34,35]), are shown in Figure 3. As expected, treatment with FBS resulted in a dose-dependent increase in matrix cell number in the attached matrix, while having little effect in the released matrix (Figure 3a). Treatment with PFT-μ resulted in a dose-dependent decrease in matrix cell number in the attached matrix, while having less pronounced effect in the released matrix (Figure 3b).

In order to compare the results of 200+ experiments similar to those shown in Figure 3, each experimental outcome first was classified according to the reagent effect on matrix cell number (data shown in Supplementary Table S10). Reagent effect in a given experiment was classified as one of the following: (1) strong inhibition, or >20% decrease in cell/matrix from the control value (control = no reagent, solvent addition only); (2) weak inhibition, or 5–20% decrease in cell/matrix from control; (3) minimal effect, or <5% change in cell/matrix from control; (4) weak stimulation, or 5–20% increase in cell/matrix from control; and (5) strong stimulation, or >20% increase in cell/matrix from control.

FBS treatment in Figure 3a demonstrated strong stimulation in the attached matrix at 72 h, while having minimal effect in the released matrix. In contrast, PFT-μ treatment demonstrated strong inhibition in the attached matrix at 72 h while having minimal effect in the released matrix (Figure 3b). Note that for each matrix condition (attached or released), two time points (48 and 72 h) were assayed, but only one outcome was reported (done to simplify the analysis). For each pair of time points, the one with the greater effect was defined as the outcome for that experiment.

The outcomes of all experiments of reagent effect in the attached *vs.* released matrix were scored as described above, and histograms of the scores for each reagent/reagent combination were constructed and plotted in Figure 4. In three experiments, the reagent effect at 48 *vs.* 72 h was exactly opposite (e.g., weak inhibition *vs.* weak stimulation); consequently, these three experiments (involving different reagents) were not included in Figure 4. An immediate observation from Figure 4 is that the results for any individual reagent

Table 4 | Select putative networks modulated between the attached *vs.* released state of the FPCM at the 6 and 24 h time points

	No.	Major participants	Relevant functions
6 h networks	6-1	TGF-β1, NF-κB, PDGF	Cellular assembly & organization; cell death
	6-2	IL-6, PCNA, cyclin A	Cell cycle
	6-3	p38, MAPK, Akt	Gene expression; tissue morphology
	6-4	SP1, CDKN2A, ErbB2	Cellular movement; cell death
	6-5	p53, PPARGC1A, EP300	Gene expression; lipid metabolism; small molecule biochemistry
24 h networks	24-1	IL-6, cyclins, CDC2	Cancer; cell cycle
	24-2	NF-κB, IL-1, RIPK2	Cell-cell signaling
	24-4	Hsp70, RNA pol II, histone H3	Cell death; gene expression
	24-5	p38, IL-8, Jnk, NF-κB	Cell growth & proliferation
	24-12	Myc, E2f	Cell cycle
	24-15	p53, NOS3	Cell cycle; DNA replication, recombination, & repair; cell death

Networks were identified with IPA® 6 analysis of DE genes. All networks identified at 6 and 24 h are shown in Supplementary Figure S8.

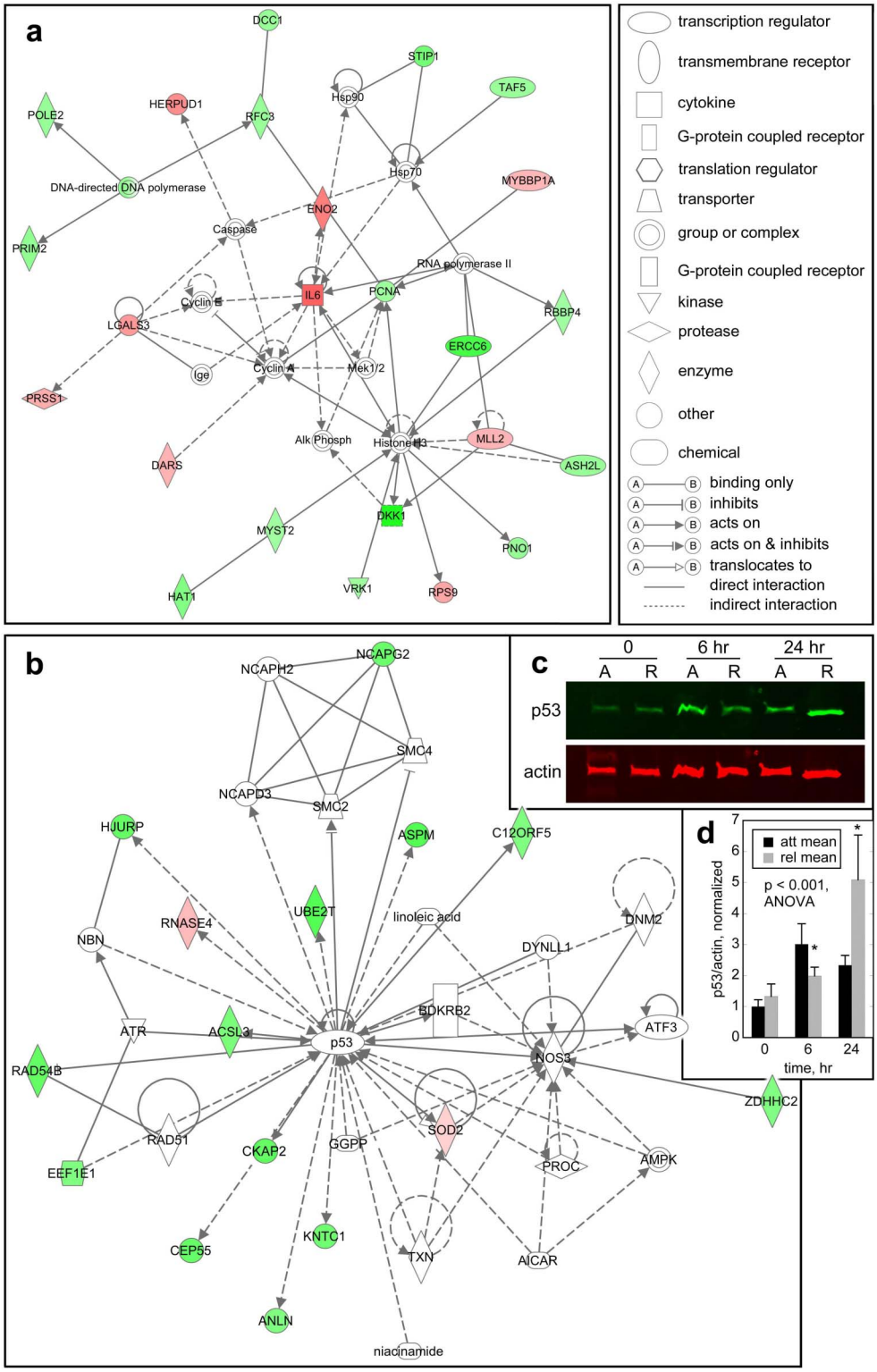

Figure 2 | Sample networks involving IL6 and p53. Putative networks modulated between the attached *vs.* released states of the FPCM were identified using IPA® 6 analysis of the microarray data. The two networks shown in the Figure were selected from the entire group of networks illustrated in Supplementary Figure S8 (see also summary in Table 4). Genes or gene products are represented as nodes (polygons). A biological relationship between two nodes is represented as an edge (line). All edges are supported by published data; see Figure key for definitions of nodes and edges. A qualitative inverse relationship exists between the edge length and the strength of the relationship (i.e., shorter edge = stronger relationship). Red or green nodal color denotes a DE gene, and indicates either gene upregulation or downregulation, respectively, in the released with respect to the attached matrix. The intensity of nodal color represents the relative difference in gene expression between attached *vs.* released; for actual mean fold change, see Supplementary Tables S1 and S2. Nodes without color were not DE genes. (A) Network 6-2; refer to Table 4. (B) Network 24-15 (refer to Table 4). (C) Immunoblot of p53 (with actin as a loading control) in the attached (A) *vs.* released (R) matrix, at 0, 6, and 24 hr after matrix release. (D) Densitometry of p53 immunoblots, with actin as the loading control. Each bar represents mean p53/actin ratio ± sd of three representative blots, normalized to the attached, t = 0 value. *$p < 0.05$ compared to attached at same time point, unpaired t-test.

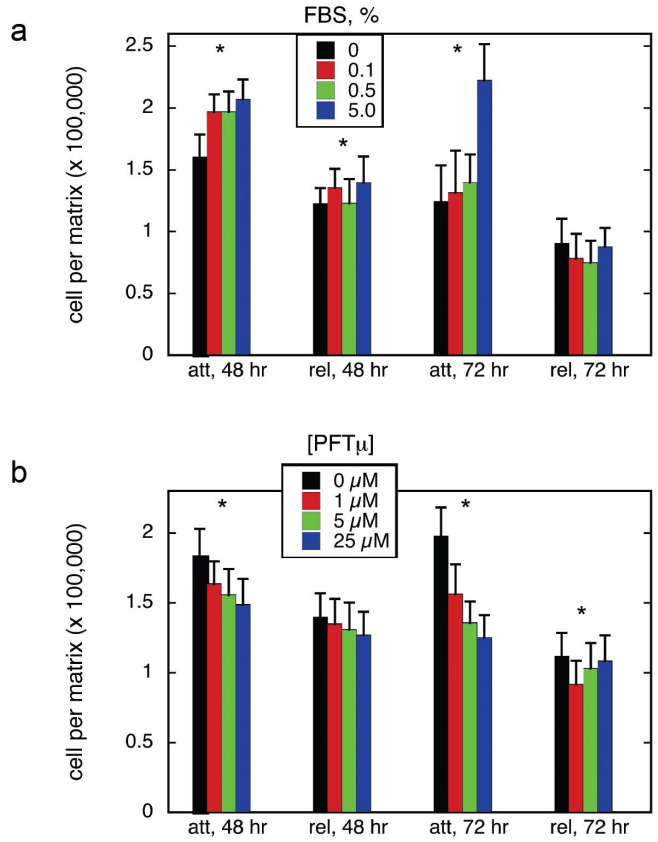

Figure 3 | Effect of FBS or PFT-μ on matrix cell number in the attached *vs.* released FPCM. Attached matrices were incubated with 5% FBS for 48–72 h. The medium then was changed (DMEM with indicated FBS concentration in panel A, and 5% FBS/DMEM in panel B), PFT-μ was added at indicated concentration for panel B, half of the matrices were released, and cell/matrix was determined 48 and 72 h later. Each bar represents the mean ± sd of 12 hemacytometer counts from a single matrix; *$p < 0.05$, ANOVA (comparing the underlying four bars).

demonstrated inter-experimental variation. For example, a plurality of experiments done with neutralizing antibody to IL6 (column 5, Figure 4) demonstrated strong inhibition, but the spread of results with anti-IL6 in 16 fibroblast strains ran from strong inhibition to strong stimulation.

Overall, most reagents appeared to have an inhibitory effect on matrix cell number, as evident from the predominance of left-shifted histograms (i.e., tall red data bars) in Figure 4. This raises the possibility of a systematic bias in the experimental design or assays. Treatment with FBS (column 1, Figure 4), however, resulted in stimulation of matrix cell number, particularly in the attached matrix. In addition, treatment with IgG (column 8, Figure 4) tended toward weak to minimal effect in most experiments. So not all reagents had an inhibitory effect.

Interestingly, both neutralization and augmentation of IL6 and/or IL8 (columns 2–8, Figure 4) resulted in general inhibition of matrix cell number. At first glance, these contradictory data seemed difficult to reconcile. With further inspection, however, it can be appreciated that the inhibition was somewhat stronger with antibody neutralization of these cytokines and, in some experiments, IL6 and/or IL8 addition stimulated matrix cell number. This might be interpreted as indicating a possible role for IL6 and/or IL8 as a "counter-regulatory" cytokine, which the fibroblasts would release after matrix detachment to preserve cell survival. IL-6 is a known wound cytokine[5], but its effect on cell fate in the collagen matrix is not known. At this point, a firm conclusion regarding the role of IL6 and/or IL8 in regulating fibroblast fate after release of the collagen matrix cannot be made.

In order to examine the role of p53, the effects of two soluble p53 inhibitors, pifithrin-alpha (PFT-α) and pifithrin-mu (PFT-μ) were tested. The former is thought to be a broad inhibitor of p53 effects[36,37], while the later is thought to be a more specific inhibitor of the cell cycle effects of p53[34,35]. Treatment with either inhibitor resulted mostly (though not exclusively) in matrix cell number inhibition; the effect of PFT-μ was perhaps more pronounced in this regard (columns 10 and 11, Figure 4). This result from p53 inhibition is somewhat counter-intuitive to the canonical function of p53 as a general promoter of apoptosis and/or cell cycle arrest in various systems[38–41]. If the canonical p53 model was in operation in our system, then one might predict that inhibition of p53 with pifithrin would result in an *increase* in matrix cell number (particularly in the released matrix), not a decrease as was observed. Further studies of p53 function in the collagen matrix using other techniques are ongoing in our laboratory. Until more data has been collected, however, it is difficult to make a strong conclusion on the role of p53 in the FPCM.

The IPA® 6 analysis generated multiple TGF-β-centric networks (numbers 6-1, 24-9, 24-10, and 24-13 in Supplementary Figure S8). Interestingly, none of the TGF-β isoforms were on DE gene lists (Supplementary Tables S1 and S2). TGF-β1 is a heavily-studied cytokine with pleiotropic, context-dependent effects; in the wound healing literature, TGF-β1 generally promotes fibrosis and fibroblast differentiation[5]. Addition of TGF-β1 to the collagen matrix model produced mostly inhibition in the attached matrix while having variable effect (from strong inhibition to strong stimulation) in the released condition (column 12, Figure 4). These results suggested that TGF-β1 may inhibit fibroblast proliferation and/or survival in the mechanically-stressed matrix. The relevance of TGF-β1 signaling in this model at this time is not clear, however, as TGF-β1 was not differentially expressed at the studied time points, and we have yet to measure TGF-β1 levels in the culture medium.

Similar to TGF-β, the software analysis identified putative networks with TNF-α or IFN-γ as central participants (networks 6-7 and 24-10, and network 24-18, respectively, in Supplementary Figure S8) yet, similar to TGF-β, neither TNF-α nor IFN-γ were differentially expressed (Supplementary Tables S1 and S2). TNF-α is another heavily-studied pleiotropic cytokine[5]; in the collagen matrix, the effect of TNF-α on cell fate is not known. Addition of TNF-α to the collagen matrix produced mostly inhibition of matrix cell number in the attached condition, with more variable effects in the released matrix (column 13, Figure 4). That is, the effects of TNF-α were similar to TGF-β1. Addition of IFN-γ to the collagen matrix also was mostly inhibitory in the attached condition, but tended toward stimulation in the released condition (column 14, Figure 4). Similar to the situation with TGF-β1, the relevance of both TNF-α and IFN-γ signaling in the collagen matrix model currently is not clear, since these were not DE genes, and endogenous cytokine levels in the collagen matrix model have yet to be assayed (with the exception of the immunoblotting shown in Supplementary Figure S11).

Three networks with NF-κB as a central participant also were identified by the software analysis (networks 6-1, 24-2, and 24-5 in Supplementary Figure S8). Of note, NF-κB was not a DE gene in the present study (Supplementary Tables S1 and S2), but other investigators have shown that NF-κB activation occurs in contractile collagen gels (analogous to the released matrices in our model)[42,43]. Similar to p53, control of NF-κB activity primarily occurs at the posttranslational level[44]. In order to determine whether NF-κB activation occurred in our version of the collagen matrix model, immunoblotting for the phosphorylated p65 subunit (Ser 536) of NF-κB was performed (Figure 5). In this example there was evidence of NF-κB activation at 10 and 30 min after matrix release.

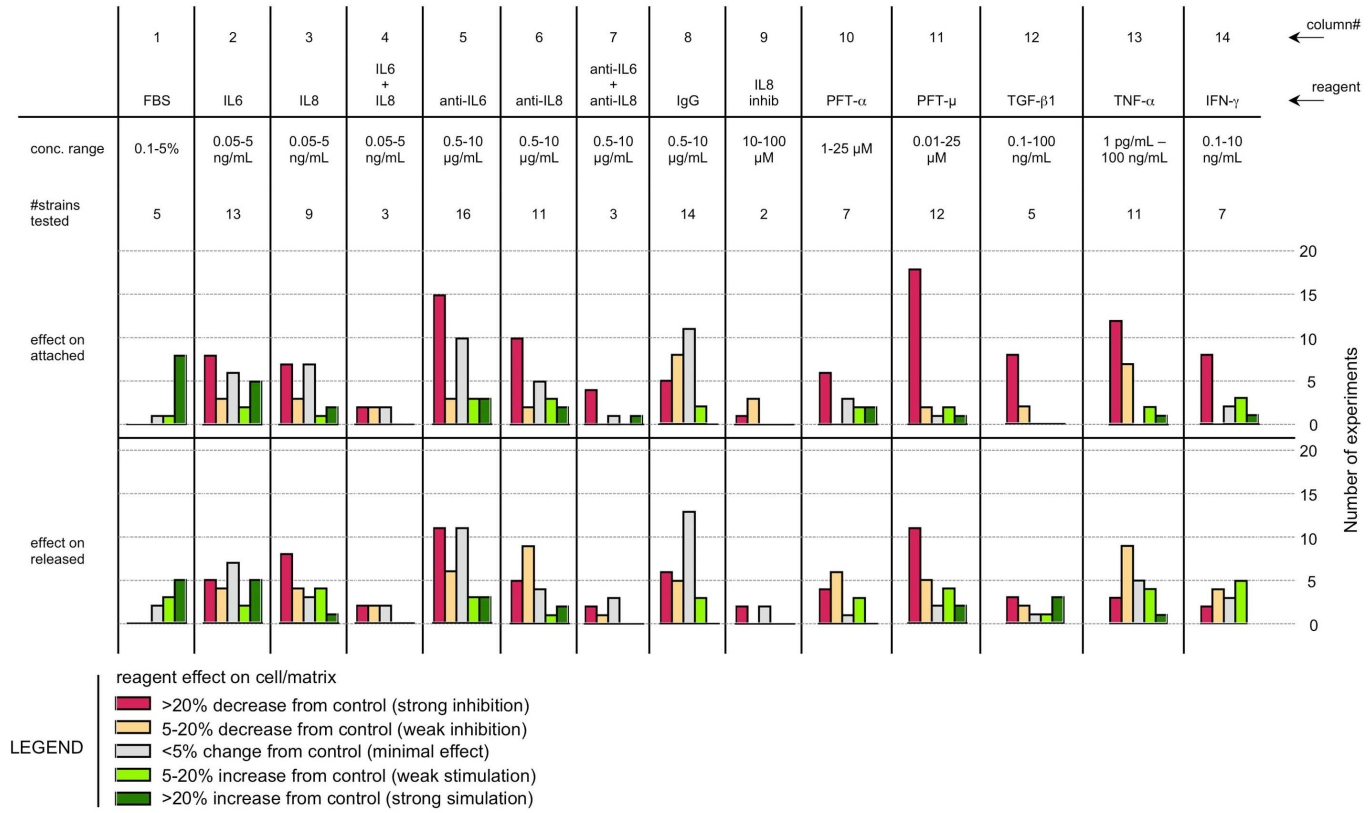

Figure 4 | Summary of effects of various soluble factors on matrix cell number in the attached *vs.* released FPCM. Matrices were handled as described in Figure 3. All experiments were done in the presence of 5% FBS (except for the experiments testing FBS itself). Each reagent/reagent combination was tested at the indicated concentration range in each of the specified number of fibroblast strains. The outcome of each experiment was scored according to the rule shown in the Figure Legend, and the a histogram of outcomes for each reagent/reagent combination was constructed for both the attached and released conditions.

Immunoblotting for p65 was repeated in attached *vs.* released matrices using five different fibroblasts strains using slightly different time course (data not shown), and the results were consistent with Figure 5. Similar immunoblotting for phospho-IκB-α (Ser 32) and IκB kinase (phospho-IKKα/b, Ser 176/180) did not reveal changes in the respective phospho-proteins after matrix release, but the signal-to-noise ratio on these blots was poor (data not shown).

As described above, treatment with TNF-α (a known inducer of NF-κB activation[45]) produced inhibition of matrix cell number in the attached condition; the effect of TNF-α in the released matrix was variable. The predominant inhibition of TNF-α in the attached matrix was consistent with the hypothesis that NF-κB activation after matrix release participates in the downregulation of matrix cell number after matrix release. Since TNF-α is a pleiotropic cytokine and may have had other effects in this model, further experimentation with augmentation or disruption of NF-κB signaling is ongoing in our laboratory to clarify the role of NF-κB in the collagen matrix.

Discussion

The data of this report are relevant to the phenomena of inflammation, wound healing, fibrosis, and related processes, because growth or regression of associated fibroblasts can influence the outcome of these phenomena[46–48]. For example, in the fields of tissue engineering or biomaterials, engendering an appropriate host response to an implanted graft or material is essential to get incorporation without foreign body reaction or rejection[49–52]. One important component of this response is the relative fibroplasia, as an excess or deficiency can lead to a poor outcome[7,50,53]. A focus on signaling networks that can regulate fibroblast fate in a native 3D extracellular matrix should provide relevant information in this regard. We are not suggesting that the information gained from this work will directly improve wound healing *in vivo*. More precisely, this work builds on the foundation of knowledge regarding cellular signaling in a 3D matrix, and the mechanoregulation of cell population within the matrix. Evolution in our understanding of these mechanisms ultimately should, however, improve our ability to manipulate wound healing, tissue engineering, endogenous regeneration, and related phenomena, as local mechanical environment can affect all of these processes[54–56].

The goal of this report was to identify signaling networks associated with the downregulation of matrix cell number as the FCPM transitions from a physically attached state to a stress-released state, with an initial relevance screen of putative networks modulated between the two mechanical states. The strengths of this report included the use of a broad screening test (DNA arrays) to identify putative networks, and the use of multiple fibroblast strains (particularly in the inhibitor/activator studies) to reduce sampling error. Some of the novel findings in this report include possible roles for IL6, IL8, NF-κB, TNF-α, TGF-β1, p53, and IFN-γ in the regulation of human foreskin fibroblast number within the 3D collagen matrix. It was not our goal in the present report to study contraction, migration, collagen synthesis, or other FPCM phenomena other than the modulation of matrix cell number after stress-release. Furthermore, the inter-relationships among mechanical force generation, contraction, and cellular fate cannot be determined without intensive experimentation, which would be beyond the scope of the present manuscript. For a discussion of how our data compared with previously published array data in the FPCM, please see Supplementary Figure S7.

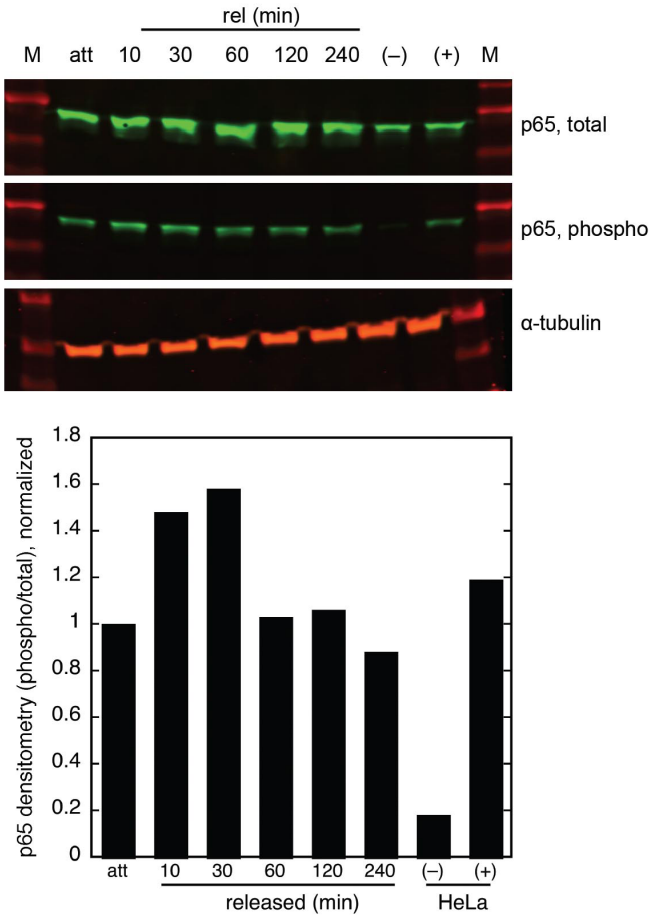

Figure 5 | NF-κB blotting in the attached *vs.* released FPCM. Attached matrices were incubated with 5% FBS for 48 h. Immunoblot of total p65, phospho-p65, and tubulin in whole lysates of attached (att) *vs.* released (rel) fibroblast-populated 3D collagen matrices at 10–240 min after release. This particular experiment was performed in five different cells strains with dissimilar time courses; thus one representative experiment without mean densitometry values is shown. HeLa (+) or (−) refers to the control HeLa cell lysate with or without pretreatment with TNF-α, respectively. The densitometry values (phospho-p65/total p65) in the bar plot were normalized to the attached value.

Three mechanical states of the collagen matrix model often are described: attached, stress-released, or floating[3]. This report only dealt with the first two states. A "floating" collagen matrix refers to a matrix which is immediately released from the culture well after polymerization (i.e., without time to develop significant pre-stress). Previous investigation has demonstrated that stress-release is a different phenomenon from matrix release immediately after polymerization, particularly with respect to contraction and intracellular signaling[57–60]. As mentioned above, the data of this report only apply to attached *vs.* stress-released matrices, and no conclusions can be drawn in this report regarding the floating matrix. It was not our intent in this report to study the differences in stress-released *vs.* floating matrices. An excellent question to pose in this respect is whether the stress-released matrix is more clinically-relevant than the floating matrix (or *vice versa*) in studying mechanoregulation within the 3D matrix. Unfortunately, debate on this question would be constrained to utilize intuitive reasoning, since there is insufficient hard evidence to support an answer.

Although use of the gene array as a screen may be seen as a strength, this technique also can be a weakness. Using gene expression may have overlooked some important signaling events in which detectable changes in mRNA concentration did not occur (e.g., post-translational events). For example, previous work referenced in the Introduction documented that disruption of pathways involving phosphorylation events (e.g., MAPK, FAK, PTEN) regulates survival in the collagen matrix. Networks predominately involving phosphorylation events may be difficult to detect with a gene expression screen. Interestingly, some of the generated networks in Supplementary Figure S8 (numbers 6-3, 24-3, 24-7) involved the PI3K-Akt axis, suggesting that phospho-signaling through this axis may have effected changes in gene expression from which the involvement of the axis could be deduced. Screening strategies which might have supplemented the DNA array data in this study would have included proteomics, kinase arrays, and RNAi screens.

Other limitations of this report included: (1) only two time points for both the DNA arrays and the inhibitor/activator studies—many important signaling may have been missed; (2) the use of a single proprietary software to generate the putative signaling networks; (3) the choice of a single endpoint (matrix cell number) in the activator/inhibitor studies, as opposed to studying endpoints such as apoptosis, proliferation, contraction, migration, collagen synthesis, etc.; and (4) the use of a single technique (small soluble mediators) to probe putative signaling networks, as opposed to using multiple techniques (such as isotype overexpression, RNAi, decoy receptors, etc.). Ongoing work in our laboratory is employing additional techniques, particularly with respect to items 3 and 4.

Matrix cell number (i.e., number of cells per matrix) was chosen as an endpoint in inhibitor/activator studies because of its simplicity[61]. While a measure of cells per matrix does not yield specific information on apoptotic or cell cycle activity, the trend in matrix cell number over time can be interpreted as a summation of the combined effects of cell death and proliferation in a closed system, such as the one under study. Matrix cell number was rapid and easy to obtain, and arguably was more relevant than individual measures of cell death or proliferation, since matrix cell number measured the net effect of multiple determinants on cell fate. Further work will include the use of endpoints such as cellular survival and proliferation.

The choices in the experimental design which led to the above (and multiple other) limitations were made to keep the study reasonably-sized. Secondary to these limitations, this report was not intended to be a finished analysis of the signaling events that occur after release of the attached collagen matrix. Therefore, none of the analyses shown in this manuscript should be taken as final; no definitive conclusions were intended to be drawn. In addition, there were many putative networks that were not even mentioned. Overall, this study was intended to be a framework by which additional studies may be planned.

Nearly all of the experiments in this report were done in the presence of serum, because (1) it has been our convention to use serum in experiments when modeling the acute wound; (2) the index microarray experiments and the derived signaling networks were the result of experiments with serum; and (3) the *in vivo* acute wound environment, which the FPCM attempts to model, contains serum-derived factors and products of platelet activation[62]. It is not clear at this time whether use of a defined, serum-free medium in the collagen matrix model would produce more biologically-relevant data than using serum-supplemented medium.

With regard to the issue of data scatter associated with the use of human foreskin fibroblasts in the collagen matrix, possible causes have been discussed previously[33]. The bottom line is that the investigator should expect this variability, and so should obtain adequate experimental repeats with multiple cell strains (a sufficient number is difficult to specify). The investigator then should be conservative about constructing conclusions from the resultant data, particularly if there is a large amount of data scatter.

It may be simplistic to view the software-generated signaling networks (Figure 2 and Supplementary Figure S8) as isolated phenomena; this would be counter to decades of signaling research.

For instance, individual entities such as p53, IL6, IL8, TGF-β1, TNF-α and INF-γ each were implicated as a central participant in at least one network in this report. In actuality, a molecule such as p53 has been shown to (i) regulate IL-6 and IL-8 expression[63–65], (ii) cooperate with SMADs in TGF-β1 signaling[66], (iii) facilitate sensitivity to TNF-α signaling[67], and (iv) undergo modulation of transcriptional activity by IFN-γ[68]. The layers of network crosstalk and other interactions of these molecules get deeper as one probes further into the literature. So the data of this report really just begin to uncover the complexities of signaling in the system under study. Ultimately, it may be determined that the reductionist approach[69] to documenting these signaling networks (as utilized in many studies, including this one) is inefficient and even inappropriate.

Regarding the mechanism of effect of the soluble inhibitors/activators used in Figure 4, it is not clear whether a given soluble mediator directly rendered its effect on matrix cell number, and/or indirectly through an effect on force generation, or through some other mechanism. In the collagen matrix model, force generation may be measured directly with specialized equipment[70] but, more typically, force generation has been studied indirectly with contraction assays[57]. As stated in the Introduction, cellular survival and proliferation in the collagen matrix is subject to mechanoregulation, so perturbation of the matrix's mechanical state (e.g., by inhibition of contraction with a soluble mediator) might effect cellular fate. Indeed, it is likely that at least some of soluble mediators used in this report (Figure 4) did affect force generation and matrix contraction. Unfortunately, the inter-relationships among mechanical force generation, contraction, and cellular fate cannot be determined without intensive experimentation, and this would be beyond the scope of the present report.

Methods

Human and animal studies. The use of primary human fibroblasts from anonymous donors (no subject identifiers and no informed consent) without the use of informed consent was approved by the Institutional Review Board at the University of Nebraska Medical Center and by the Research and Development Committee at the Omaha VA Medical Center. The use of animals was approved by the Subcommittee of Animal Studies and by the Research and Development Committee (protocols 00248 and 00457) at the Omaha VA Medical Center.

Design of index experiment: expression analysis of attached vs. released collagen matrices. The following information on the microarrays was supplied per the standards of the Minimum Information About a Microarray Experiment workgroup (MIAME 2.0, www.mged.org)[71,72]. The index microarray experiment (see flow diagram in Supplementary Figure S5) was performed three times, each time using cells from a unique individual (i.e., three separate strains of primary fibroblasts, defined as F1, F2, and F3). The list of DE genes in Supplementary Tables S1 and S2 are derived from these three index experiments. For a given index experiment, collagen matrices (six matrices per group, four groups of six matrices per index experiment, as shown in Supplementary Figure S5) were set up as described in the preceding section, and incubated in the attached state in growth medium for 24 h. Two of the four groups of matrices then were mechanically released from the culture dish. One attached group and one released group subsequently underwent RNA extraction at 6 h and then at 24 h post-release (Supplementary Figure S5). To reiterate, the index experiment shown in Supplementary Figure S5 was performed on three separate strains of foreskin fibroblasts.

RNA extraction and aRNA synthesis. Immediately after completion of incubation, each group of collagen matrices was washed with PBS and then homogenized (Ultra-Turrax® T25; IKA® Laboratories) in a glass tube with 600 μL Buffer RLT (Qiagen®) supplemented with 1% β-mercaptoethanol. RNA then was isolated from the homogenized samples using a proprietary kit (RNeasy® Mini Kit; Qiagen®), following the recommendations of the manufacturer. The purity of the extracted RNA was checked with spectrophotometry (Bioanalyzer 2100; Agilent Technologies) and agarose electrophoresis. Only intact and pure samples ($A_{260}/A_{280} > 1.8$, with distinct electrophoretic bands) were used for labeling. Processing and Cy5/Cy3 labeling of RNA samples were performed using the Message Amp aRNA kit (Ambion). Total RNA (1 μg) was reverse-transcribed, and the resultant cDNA was used to generate aRNA using an *in vitro* transcription procedure per the manufacturer's recommendation. The Cy5 and Cy3 labels were applied to the released and attached aRNA, respectively; by convention, the attached matrix was denoted as the baseline or reference condition.

DNA microarrays. The aRNA was hybridized to 10 K spotted arrays produced at the UNMC DNA Microarray Core facility (a complete list of genes is available in Gene Expression Omnibus, accession number GSE39475). To reiterate, the total number of arrays (i.e., gene chips) used to obtain the DE genes in Supplementary Tables S1 and S2 was six, representing six attached *vs.* released hybridization pairs, generated from three separate experiments that had two attached *vs.* released time points each (see Supplementary Figure S5). The arrays were prehybridized to minimize background, followed by hybridization to the Cy3 and Cy5 probes. Following overnight hybridization, the slides were washed to remove nonspecific binding. Cy3 (532 nm) and Cy5 (635 nm) scans were performed using a GenePix 4000 b slide reader (Molecular Devises), and gene spot intensity assessment on 16 bit TIFF files was performed with the GenePix image analysis software.

Summary of design for array index experiments. Refer to Supplementary Figure S5. Four distinct treatments (6 h attached, 6 h released, 24 h attached, and 24 h released) were applied to three fibroblasts strains (F1, F2, and F3), so there were 12 independent groups of matrices (each group comprising 6 replicate matrices). The RNA from replicate matrices within a group was pooled, but RNA among groups was not pooled (i.e., RNA among fibroblast strains was not pooled). Labeled aRNA from the twelve independent samples was competitively hybridized to a total of 6 gene chips (a common reference was not used). Only attached *vs.* released comparisons were performed; chips which compared time points (e.g., 6 h attached *vs.* 24 h attached) were not done.

Analysis of expression data. BRB ArrayTools (http://linus.nci.nih.gov/BRB-ArrayTools.htmL) was used to analyze the microarray data. Prior to the analysis, several filters and normalization were applied: (1) spots were excluded if both the red and green channels had values less than 100; (2) if only one of the red or green channels had a value <100, then the value was increased to the threshold of 100; (3) median background was subtracted; (4) $\log_2$ transformation was applied to all ratios; (5) normalization was performed using the Lowess smoother; (6) a gene was excluded if 3 of its spots were missing or filtered out. Random-variance paired t-testing was used to determine which genes were differentially expressed between the released and attached groups. The random-variance paired t-test allows sharing information among genes about variation without assuming that all genes have the same variance, which gives a more accurate estimate of the variability when sample sizes are small[73]. Distributional assumptions were checked using the Kolmogorov Goodness-of-Fit Test[74]. The distributional assumptions of the random-variance test were met for the paired testing (6 and 24 hour time points separately comparing released vs. attached groups). Conventional t-testing was utilized to compare the relative changes between the 6 and 24 h time points; the random-variance t-test was not used in this latter situation because of violations of distribution assumptions. A significance level of 0.001 was selected in these analyses to help limit the false discovery rate due to multiple comparisons. Benjamini-Hochberg false discovery rate method (FDR) also was used to correct p-values, and the adjusted FDR values are given in Supplementary Tables S1 and S2[75]. Additional screening using a two-fold change cutoff was employed to focus on genes which had a biologically meaningful change in expression. To reiterate, a differentially-expressed gene (Supplementary Tables S1 and S2) required the following: (1) relative expression of released/attached ≥ 2 or ≤ 0.5; (2) significance of $p < 0.001$; (3) false discovery rate (FDR) $< 5\%$.

Identification of relevant gene networks. Genes with a mean fold change (defined as the mean absorbance value of the gene in the released matrix divided by the mean absorbance value of the gene in the attached matrix) of >2 or <0.5 (focus genes), with a significance < 0.001 and FDR $< 5\%$, subsequently were analyzed with Ingenuity® Pathways Analysis (IPA 6; www.ingenuity.com), a proprietary web-based program that can identify gene networks potentially modulated in sets of expressional data (see further description under Results)[27,28]. A dataset of focus gene identifiers with their corresponding attached *vs.* released expression value were uploaded into the program as a Microsoft® Excel® spreadsheet, using a template supplied by Ingenuity® Systems. Each focus gene identifier was mapped to its corresponding gene object in the Ingenuity Pathways Knowledge Base. The focus genes were overlaid onto a global molecular network developed from information contained in the Ingenuity Pathways Knowledge Base. Networks of these focus genes were then algorithmically generated based on their connectivity, and then graphically portrayed (see further description under Results). The program limited the number of participants in each network to 35, so that reasonable 2D illustrations could be generated (Figure 2). Note that each IPA-generated network is constructed and customized to the list of focus genes that is uploaded into the program; as such, a given IPA-generated network is unique, and may not resemble any previously-published network.

Other materials & methods. Details of cell culture, the collagen matrix model, the excisional wound model, immunoblotting, TUNEL, BrdU labeling, matrix cell number quantification, qPCR, ELISA, and statistics are supplied as a Supplementary File.

1. Bell, E., Ehrlich, H. P., Buttle, D. J. & Nakatsuji, T. Living tissue formed in vitro and accepted as skin-equivalent tissue of full thickness. *Science* **211**, 1052–1054 (1981).
2. Bell, E., Sher, S. & Hull, B. The living skin-equivalent as a structural and immunological model in skin grafting. *Scan Electron Microsc* 1957–1962 (1984).

3. Grinnell, F. Fibroblasts, myofibroblasts, and wound contraction. *J Cell Biol* **124**, 401–404 (1994).
4. Boyce, S. T., Kagan, R. J., Meyer, N. A., Yakuboff, K. P. & Warden, G. D. The 1999 clinical research award. Cultured skin substitutes combined with Integra Artificial Skin to replace native skin autograft and allograft for the closure of excised full-thickness burns. *J Burn Care Rehabil* **20**, 453 (1999).
5. Carlson, M. A. & Longaker, M. T. The fibroblast-populated collagen matrix as a model of wound healing: a review of the evidence. *Wound Repair Regen* **12**, 134–147 (2004).
6. Dallon, J. C. & Ehrlich, H. P. A review of fibroblast-populated collagen lattices. *Wound Repair Regen* **16**, 472–479 (2008).
7. Metcalfe, A. D. & Ferguson, M. W. Tissue engineering of replacement skin: the crossroads of biomaterials, wound healing, embryonic development, stem cells and regeneration. *J R Soc Interface* **4**, 413–437 (2007).
8. Yamada, K. M. & Cukierman, E. Modeling tissue morphogenesis and cancer in 3D. *Cell* **130**, 601–610 (2007).
9. Boyce, S. T. & Warden, G. Principles and Practices for treatment of cutaneous wounds with cultured skin substitutes. *Am J Surg* **183**, 445–456 (2002).
10. Badylak, S. F., Taylor, D. & Uygun, K. Whole-organ tissue engineering: decellularization and recellularization of three-dimensional matrix scaffolds. *Annu Rev Biomed Eng* **13**, 27–53 (2011).
11. Grinnell, F., Zhu, M., Carlson, M. A. & Abrams, J. M. Release of Mechanical Tension Triggers Apoptosis of Human Fibroblasts in a Model of Regressing Granulation Tissue. *Exp Cell Res* **248**, 608–619 (1999).
12. Hadjipanayi, E., Mudera, V. & Brown, R. Close dependence of fibroblast proliferation on collagen scaffold matrix stiffness. *J Tiss Eng Regen Med* **3**, 77–84 (2009).
13. Fluck, J. *et al*. Normal human primary fibroblasts undergo apoptosis in three-dimensional contractile collagen gels. *J Invest Dermatol* **110**, 153–157 (1998).
14. Rosenfeldt, H. & Grinnell, F. Fibroblast quiescence and the disruption of ERK signaling in mechanically unloaded collagen matrices. *J Biol Chem* **275**, 3088–3092 (2000).
15. Fringer, J. & Grinnell, F. Fibroblast quiescence in floating or released collagen matrices: contribution of the ERK signaling pathway and actin cytoskeletal organization. *J Biol Chem* **276**, 31047–31052 (2001).
16. Fringer, J. & Grinnell, F. Fibroblast quiescence in floating collagen matrices: decrease in serum activation of MEK and Raf but not Ras. *J Biol Chem* **278**, 20612–20617 (2003).
17. Tian, B., Lessan, K., Kahm, J., Kleidon, J. & Henke, C. beta 1 integrin regulates fibroblast viability during collagen matrix contraction through a phosphatidylinositol 3-kinase/Akt/protein kinase B signaling pathway. *J Biol Chem* **277**, 24667–24675 (2002).
18. Xia, H., Nho, R. S., Kahm, J., Kleidon, J. & Henke, C. A. Focal adhesion kinase is upstream of phosphatidylinositol 3-kinase/Akt in regulating fibroblast survival in response to contraction of type I collagen matrices via a beta 1 integrin viability signaling pathway. *J Biol Chem* **279**, 33024–33034 (2004).
19. Nho, R. S. *et al*. PTEN regulates fibroblast elimination during collagen matrix contraction. *J Biol Chem* **281**, 33291–33301 (2006).
20. Nho, R. S. *et al*. Role of integrin-linked kinase in regulating phosphorylation of Akt and fibroblast survival in type I collagen matrices through a beta1 integrin viability signaling pathway. *J Biol Chem* **280**, 26630–26639 (2005).
21. Grinnell, F. & Petroll, W. M. Cell motility and mechanics in three-dimensional collagen matrices. *Annu Rev Cell Dev Biol* **26**, 335–361 (2010).
22. Eckes, B. *et al*. Mechanical tension and integrin alpha 2 beta 1 regulate fibroblast functions. *J Invest Dermatol* **11**, 66–72 (2006).
23. Carlson, M. A., Longaker, M. T. & Thompson, J. S. Granulation tissue regression induced by musculocutaneous advancement flap coverage. *Surgery* **131**, 332–337 (2002).
24. Carlson, M. A. & Thompson, J. S. Wound splinting modulates granulation tissue proliferation. *Matrix Biol* **23**, 243–250 (2004).
25. Carlson, M. A. & Thompson, J. S. Wound matrix attachment regulates actin content and organization in cells of the granulation tissue. *Wound Repair Regen* **13**, 84–92 (2005).
26. Carlson, M. A., Eudy, J. D., Smith, L. M. & Gums, J. J. Gene expression in attached vs. released collagen matrices populated with human foreskin fibroblasts. NCBI Gene Expression Omnibus, 2012, Acc No. GSE39475 (http://www.ncbi.nlm.nih.gov/geo/query/acc.cgi?acc=GSE39475). Date accessed: July 19, 2012.
27. Rajagopalan, D. & Agarwal, P. Inferring pathways from gene lists using a literature-derived network of biological relationships. *Bioinformatics* **21**, 788–793 (2005).
28. Calvano, S. E. *et al*. A network-based analysis of systemic inflammation in humans. *Nature* **437**, 1032–1037 (2005).
29. Dey, A., Verma, C. S. & Lane, D. P. Updates on p53: modulation of p53 degradation as a therapeutic approach. *Br J Cancer* **98**, 4–8 (2008).
30. Brooks, C. L. & Gu, W. Ubiquitination, phosphorylation and acetylation: the molecular basis for p53 regulation. *Curr Opin Cell Biol* **15**, 164–171 (2003).
31. Gu, B. & Zhu, W. G. Surf the post-translational modification network of p53 regulation. *Int J Biol Sci* **8**, 672–684 (2012).
32. Kruse, J. P. & Gu, W. Modes of p53 regulation. *Cell* **137**, 609–622 (2009).
33. Carlson, M. A., Prall, A. K., Gums, J. J., Lesiak, A. & Shostrom, V. K. Biologic variability of human foreskin fibroblasts in 2D and 3D culture: implications for a wound healing model. *BMC Res Notes* **2**, 229 (2009).
34. Strom, E. *et al*. Small-molecule inhibitor of p53 binding to mitochondria protects mice from gamma radiation. *Nat Chem Biol* **2**, 474–479 (2006).
35. Green, D. R. & Kroemer, G. Cytoplasmic functions of the tumour suppressor p53. *Nature* **458**, 1127–1130 (2009).
36. Komarova, E. A. *et al*. p53 inhibitor pifithrin alpha can suppress heat shock and glucocorticoid signaling pathways. *J Biol Chem* **278**, 15465–15468 (2003).
37. Culmsee, C. *et al*. A synthetic inhibitor of p53 protects neurons against death induced by ischemic and excitotoxic insults, and amyloid beta-peptide. *J Neurochem* **77**, 220–228 (2001).
38. Zhang, X. P., Liu, F., Cheng, Z. & Wang, W. Cell fate decision mediated by p53 pulses. *Proc Natl Acad Sci* **106**, 12245–12250 (2009).
39. Speidel, D. Transcription-independent p53 apoptosis: an alternative route to death. *Trends Cell Biol* **20**, 14–24 (2010).
40. Vazquez, A., Bond, E. E., Levine, A. J. & Bond, G. L. The genetics of the p53 pathway, apoptosis and cancer therapy. *Nat Rev Drug Disc* **7**, 979–987 (2008).
41. Purvis, J. E. *et al*. p53 dynamics control cell fate. *Sci Signal* **336**, 1440 (2012).
42. Xu, J. & Clark, R. A. A three-dimensional collagen lattice induces protein kinase C-zeta activity: role in alpha2 integrin and collagenase mRNA expression. *J Cell Biol* **136**, 473–483 (1997).
43. Xu, J., Zutter, M. M., Santoro, S. A. & Clark, R. A. A three-dimensional collagen lattice activates NF-kappaB in human fibroblasts: role in integrin alpha2 gene expression and tissue remodeling. *J Cell Biol* **140**, 709–719 (1998).
44. Baltimore, D. NF-kappaB is 25. *Nature Immunol* **12**, 683–685 (2011).
45. Ruland, J. Return to homeostasis: downregulation of NF-kappaB responses. *Nature Immunol* **12**, 709–714 (2011).
46. Epstein, F. H., Singer, A. J. & Clark, R. A. F. Cutaneous wound healing. *New Engl J Med* **341**, 738–746 (1999).
47. Park, J. E. & Barbul, A. Understanding the role of immune regulation in wound healing. *Am J Surg* **187**, S11–S16 (2004).
48. Steed, D. L. Wound-healing trajectories. *Surg Clin N Am* **83**, 547 (2003).
49. Eming, S. A., Krieg, T. & Davidson, J. M. Inflammation in wound repair: molecular and cellular mechanisms. *J Invest Dermatol* **127**, 514–525 (2007).
50. Anderson, J. M., Rodriguez, A. & Chang, D. T. Foreign body reaction to biomaterials. *Semin Immunol* **20**, 86–100 (2008).
51. Jones, K. S. Effects of biomaterial-induced inflammation on fibrosis and rejection. *Semin Immunol* **20**, 130–136 (2008).
52. Ikada, Y. Challenges in tissue engineering. *J R Soc Interface* **3**, 589–601 (2006).
53. Nolte, S. V., Xu, W., Rennekampff, H. O. & Rodemann, H. P. Diversity of fibroblasts—a review on implications for skin tissue engineering. *Cells Tiss Org* **187**, 165–176 (2008).
54. Tomasek, J. J., Gabbiani, G., Hinz, B., Chaponnier, C. & Brown, R. A. Myofibroblasts and mechano-regulation of connective tissue remodelling. *Nat Rev Mol Cell Biol* **3**, 349–363 (2002).
55. Nagel, T. & Kelly, D. J. Mechano-regulation of mesenchymal stem cell differentiation and collagen organisation during skeletal tissue repair. *Biomech Model Mechanobiol* **9**, 359–372 (2010).
56. Kelly, D. & Prendergast, P. J. Mechano-regulation of stem cell differentiation and tissue regeneration in osteochondral defects. *J Biomechan* **38**, 1413–1422 (2005).
57. Grinnell, F. Fibroblast biology in three-dimensional collagen matrices. *Trends Cell Biol* **13**, 264–269 (2003).
58. Grinnell, F. & Ho, C. H. Transforming growth factor beta stimulates fibroblast-collagen matrix contraction by different mechanisms in mechanically loaded and unloaded matrices. *Exp Cell Res* **273**, 248–255 (2002).
59. Grinnell, F. Fibroblast-collagen-matrix contraction: growth-factor signalling and mechanical loading. *Trends Cell Biol* **10**, 362–365 (2000).
60. Grinnell, F., Ho, C. H., Lin, Y. C. & Skuta, G. Differences in the regulation of fibroblast contraction of floating versus stressed collagen matrices. *J Biol Chem* **274**, 918–923 (1999).
61. Carlson, M. A. Technical note: assay of cell quantity in the fibroblast-populated collagen matrix with a tetrazolium reagent. *Eur Cell Mater* **12**, 44–48 (2006).
62. Shaw, T. J. & Martin, P. Wound repair at a glance. *J Cell Sci* **122**, 3209–3213 (2009).
63. Jin, S. *et al*. Non-canonical Notch signaling activates IL-6/JAK/STAT signaling in breast tumor cells and is controlled by p53 and IKKα/IKKβ. *Oncogene* Nov 26, 2012. doi: 10.1038/onc.2012.517. [Epub ahead of print]
64. Margulies, L. & Sehgal, P. Modulation of the human interleukin-6 promoter (IL-6) and transcription factor C/EBP beta (NF-IL6) activity by p53 species. *J Biol Chem* **268**, 15096–15100 (1993).
65. Khwaja, F. *et al*. Proteomic identification of the wt-p53-regulated tumor cell secretome. *Oncogene* **25**, 7650–7661 (2006).
66. Cordenonsi, M. *et al*. Links between tumor suppressors: p53 is required for TGF-Œ≤ gene responses by cooperating with Smads. *Cell* **113**, 301–314 (2003).
67. Klefstrom, J. *et al*. Induction of TNF-sensitive cellular phenotype by c-Myc involves p53 and impaired NF-Œ∫B activation. *The EMBO journal* **16**, 7382–7392 (1997).
68. Ossina, N. K. *et al*. Interferon-gamma modulates a p53-independent apoptotic pathway and apoptosis-related gene expression. *J Biol Chem* **272**, 16351–16357 (1997).
69. Ahn, A. C., Tewari, M., Poon, C.-S. & Phillips, R. S. The limits of reductionism in medicine: could systems biology offer an alternative? *PLoS Med* **3**, e208 (2006).

70. Eastwood, M., Porter, R., Khan, U., McGrouther, G. & Brown, R. Quantitative analysis of collagen gel contractile forces generated by dermal fibroblasts and the relationship to cell morphology. *J Cell Physiol* **166**, 33–42 (1996).
71. Brazma, A. *et al.* Minimum information about a microarray experiment (MIAME)-toward standards for microarray data. *Nat Genet* **29**, 365–371 (2001).
72. Editorial. Minimum compliance for a microarray experiment? *Nat Genet* **38**, 1089 (2006).
73. Wright, G. W. & Simon, R. M. A random variance model for detection of differential gene expression in small microarray experiments. *Bioinformatics* **19**, 2448–2455 (2003).
74. Conover, W. J. *Practical Nonparametric Statistics*, 2nd Ed. (John Wiley & Sons, Inc., 1980).
75. Benjamini, Y. & Hochberg, Y. Controlling the false discovery rate: a practical and powerful approach to multiple testing. *J R Stat Soc Ser B* **57**, 289–300 (1995).

Acknowledgments

This work was supported with resources and the use of facilities at the Omaha VA Medical Center. The authors would like to make the following acknowledgements: Chris Hansen, Dean Heimann, Amy Prall, J.J. Gums, and Lisa Bough for technical assistance; Charles Kuszynski, Linda Wilkie, and Victoria Smith for flow cytometry support; and Debra Romberger and Art Heires for performance of the ELISAs. The first author also would like to express his appreciation for helpful discussions with Fred Hamel, Bob Bennett, Courtney Schaffert, Jie Chao, Chris Eischen, Fred Grinnell, and Angie Rizzino. Some of the text describing the IPA 6 program was modified from public domain descriptions available on the Ingenuity® web site (www.ingenuity.com).

Author contributions

M.A.C. designed the experiments, analyzed the data, wrote the paper, and supervised the project; L.M.S. performed the statistical analysis of the microarray data; C.M.C. performed experiments and analyzed the data; J.C. performed experiments and analyzed the data; J.D.E. designed and supervised the microarray experiments. All authors critiqued and approved the manuscript.

Additional information

Supplementary information accompanies this paper at http://www.nature.com/scientificreports

Competing financial interests: The authors declare no competing financial interests.

How to cite this article: Carlson, M.A., Smith, L.M., Cordes, C.M., Chao, J. & Eudy, J.D. Attachment-regulated signaling networks in the fibroblast-populated 3D collagen matrix. *Sci. Rep.* **3**, 1880; DOI:10.1038/srep01880 (2013).